Journal of Medical Systems (2019) 43: 240
https://doi.org/10.1007/s10916-019-1370-x

IMAGE & SIGNAL PROCESSING

Medical Image Enhancement by a Bilateral Filter Using Optimization Technique

V. Anoop [1] · P. R. Bipin [2]

Received: 12 March 2019 / Accepted: 5 June 2019 / Published online: 20 June 2019

Abstract

For researchers, denoising of Magnetic Resonance (MR) image is a greatest challenge in digital image processing. In this paper, the impulse noise and Rician noise in the medical MR images are removed by using Bilateral Filter (BF). The novel approaches are presented in this paper; Enhanced grasshopper optimization algorithm (EGOA) is used to optimize the BF parameters. To simulate the medical MR images (with different variances), the impulse and Rician noises are added. The EGOA is applied to the noisy image in searching regions of window size, spatial and intensity domain to obtain the filter parameters optimally. The PSNR is taken as fitness value for optimization. We examined the proposed technique results with other MR images After the optimal parameters assurance. In order to comprehend the BF parameters selection importance, the results of proposed denoising method is contrasted with other previously used BFs, genetic algorithm (GA), gravitational search algorithm (GSA) using the quality metrics such as signal-to-noise ratio (SNR), structural similarity index metric (SSIM), mean squared error (MSE), and PSNR. The outcome shows that the EOGA method with BF shows good results than the earlier methods in both edge preservation and noise elimination from medical MR images. The experimental results demonstrate the performance of the proposed method with the accuracy, computational time, and maximum deviation, Peak Signal to Noise Ratio (PSNR), MSE, SSIM, and entropy values of MR images over the existing methods.

Keywords Bilateral filter · Rician and impulse noise · SNR · EGOA · Genetic algorithm · Noise elimination

Introduction

The medical image created by MRI, CT, X-ray and ultrasound assumes an essential part in the identification of diseases [1]. The distinguishing proof, examination and treatment of infections are influenced by the noises introduce in the image [2]. The noises are delivered in the images at the time of transmission and procurement because of the ecological conditions and obstruction in the channel. The temperature variations of the sensor additionally create noises [3]. The denoising of medical image is essential for the diagnosis and treatment planning process. As of late the images are caught utilizing the digital system. The evacuation of noises in the digital image is a troublesome errand [1]. The noises decrease the nature of the image. The sort of the noise ought to be distinguished and its statistical properties ought to be examined for the denoising procedure [4]. Different kinds of noises, for example, Gaussian noise, Rayleigh noise impulse noise are delivered amid the image acquisition process. The Gaussian noise and Rayleigh noise are produced amid sampling and transmission. The impulse noise is additionally called as salt and pepper noise. It happens in the image as black and white specks [5, 6]. Add up to variation filter, changing domain filter and gradient technique is a portion of the strategies utilized for image denoising. Add up to variation filters and change domain filters are influenced by finished smoothing impact [7, 8].

The noise named as Rician noise which is delivered in the MR images are evacuated utilizing the fuzzy hybrid filter. The Rician noises in the images influence the post handling procedures like segmentation and parametric synthesis [9]. The speckle noise in the ultrasound medical image is diminished

This article is part of the Topical Collection on *Image & Signal Processing*

✉ V. Anoop
vanoop@gmail.com

[1] Jyothi Engineering College, Cheruthuruthy, Thrissur, Kerala 679531, India

[2] Ilahiya College of Engineering and Technology, Muvattupuzha, Kerala, India

by unbiased non local means technique, Bayesian estimator and non-local mean filter. The unbiased non local means strategy registers the shape and scale parameters of the Gamma distribution and intensity of every pixel is figured for the denoising procedure. A monogenic wavelet contrasted and Bayesian estimator expels the noises from the images by demonstrating the noise as Laplace mixture distribution and Rayleigh distribution. The non-local mean filter denoise the image by registering the weighted average of all pixels [10–12].

Some different calculations, for example, nonlinear filters in the next years, contingent upon conditions of partial differential, AD (Anisotropic Diffusions), NLM (non-local means), wavelets and curvelet based transformation filters and statistical filters have been presented for MRI filtering with a specific end goal to beat this disadvantage of obscuring. It tends to be inferred that amid the previous year's many filtering strategies for noise have been introduced for MRI; among these methods, a famous nonlinear filter is bilateral filter. It is basic approach, local and non-iterative utilized for disposal of noise and edge preservation in spatial domain. In an image for recognizing itemized parts that utilizations local information. At that point, these segments smoothes different parts of image [13]. Despite the fact that BF is in effect broadly utilized for MRI images denoising, for the BF parameters optimal selection it has been accounted for that there isn't much hypothetical investigation [14, 15]. In past examinations, to discover optimal parameters statistical approaches were chosen. For modifying optimal filter parameters creators [16] utilized estimations of vector root mean squared error. Nonetheless, their approach accepts that a ground truth image is known. In another optimization investigation of BF parameter directed in view of PSO, color images misleadingly defiled by just a single level noise were explored for parameters of BF proposal [17]. Generally, by preliminary the BF parameters are typically decided and error by practice [18].

Enhanced Grasshopper Optimization Algorithm (EGOA) has been demonstrated to profit by high investigation while appearing quick union speed. The exceptional versatile instrument in this calculation easily balances investigation and abuse. These attributes make the EGOA calculation conceivably ready to adapt to the troubles of a multi-objective pursuit space and outflank different strategies. The computational multifaceted nature is superior to those of numerous advancement methods in the writing. These ground-breaking highlights persuaded our endeavors to propose a multi-objective streamlining agent enlivened by the social conduct of grasshoppers in nature. The contribution of this paper is to remove noise from medical MR image and optimize the BF parameters using EGOA. The EGOA approach strength is in a fast manner that it usually discovers an optimal solution to a problem with knowledge of less prior about the problem than the other methods [19]. To the best of our insight, for denoising of MR medical images this paper is the first EGOA based optimization work to find optimal BF parameters.

The expected outcome of this paper is to reduce the medical MR image Rician and impulse noise with different noise level (sd = 10, 20, 30) and estimate the optimal filter parameters using enhanced GOA for obtaining higher PSNR values significantly. Using the quality metrics and visual inspections we evaluated the proposed method on clinical and simulated medical MR images. Additionally, discuss the performance comparison of our method and other classical BFs methods. The scientific contribution of the paper is measuring the evaluation metrics and the computational time. While comparing with the existing methods the proposed method gives the better result. The structure of paper is arranged as follows; the brief review of literature work is presented in section "Related work: A brief review". Section "Proposed methodology" includes the outline of the proposed methodology. Section "Result and discussion" includes the performance evaluation and experimental results and section "Conclusion" concludes the paper.

Related work: A brief review

The process of safeguarding every relevant feature from medical MR image by evacuating noise is called denoising. For denoising reason there are various procedures are accessible some of them are reviewed here,

Kai Hu et al. [20] have shown the directional development for the undecorated wavelet transform (DEUWT) for MR image denoising. A intricate data denoising algorithm which was a combination of DEUWT and stein's impartial hazard estimator (SURE) thresholding for denoising. The presented procedure had enhanced execution when contrasted and the current strategies. Muhammad et al. [21] have introduced optimal composite morphological supervised filter and genetic programming (GP) for MR image denoising. The denoising procedure was separated into pre-processing module, GP module and assessment module. The segments required for GP based filter was registered in the pre-processing process. The execution of the presented technique had enhanced when contrasted and the current strategies.

The creators [22] built up a weighted three dimensional wavelet transform for denoising of MR images. A three dimensional discrete wavelet transform is utilized for the denoising procedure. The displayed strategy had enhanced effectiveness than the current techniques. Memoona Malik et al. [23] have planned a cuckoo search algorithm for image denoising. The Gaussian noise, speckle noise, and salt and pepper noise were decreased utilizing a hybrid smoothing filter with cuckoo search algorithm. The efficiency of the

introduced strategy was enhanced when contrasted and the current strategies.

Jonatas et al. [24] have presented a method for image denoising based on a hybrid genetic algorithm (HGA). The HGA was the blend of genetic algorithm and denoising strategies. The additive Gaussian noise and speckle noises were diminished utilizing their strategy. Their strategy had enhanced execution than the current strategies. Zhang et al. [25] have introduced a wavelet and guided filter for the evacuation of speckle noise in the medical ultrasonic pictures. The universal threshold work was utilized to acquire the threshold work. Rayleigh Distribution and generalized Gaussian distribution were utilized for displaying the wavelet coefficients. The introduced strategy was effective for the speckle noise expulsion than the current strategies.

Aref Miri et al. [26] have presented ABC algorithm (Ant Bee Colony optimization) for medical image denoising. The frequency coefficients were recognized for expelling the noises. The noises were expelled by disposing of the high frequency parts. The Gaussian noise was evacuated by their strategy. The execution of the introduced procedure was enhanced than the current strategies. H. Naimi et al. [27] have outlined a dual tree complex wavelet transform and wiener filter for medical image denoising. The shrinkage of wavelet thresholding was gotten by soft or hard thresholding system. The accuracy of the introduced strategy was enhanced when contrasted and the current techniques.

Henrick [28] implement the development identifies with a strategy for picture handling of attractive reverberation (MR) pictures for making denoised MR pictures, specifically to a technique for denoising picture information in wavelet area. An attractive reverberation imaging gadget for executing the technique is additionally revealed. Uses of the innovation are accessible in all fields of attractive reverberation imaging, specifically practical as well as quantitative restorative imaging. Sudeep [29] the article primarily centered on the upgrade of the MR greatness information, which pursue a non-stationary Rician conveyance. The proposed NLML system is dedicated to improving the ordinary NLML estimation technique by utilizing the earlier data of the evaluated commotion map utilizing a robust noise estimator and by joining the LFD-based closeness measure. The drawback is high complexity. Chen [30] Dispersion MRI (DMRI) depends on its affectability to the dislodging of water atoms to test tissue microstructure. To have the option to portray fine micro structural subtleties, the dispersion weighting (i.e., b-esteem) should be adequately high, permitting, for instance, increasingly exact partition of fiber groups crossing at little points and more noteworthy affectability to the confined dissemination of water atoms caught inside axons. Be that as it may, because of the huge lessening of the MR signal at high dispersion weightings, the low sign to-commotion proportion (SNR) presents noteworthy difficulties to consequent examination.

Proposed methodology

Outline of proposed methodology

The proposed strategy actualizes an iterative bilateral filter for denoising magnitude MR images utilizing EGOA. The famous nonlinear filter for edge-preserved denoising is bilateral filter which is employed in spatial domain. Figure 1 demonstrates the flowchart of the proposed methodology. Here, the medical images are taken as input image and add noises namely Rician noise and impulse (salt and pepper) noise with various noise variance to form noisy image. The noisy image is denoised utilizing bilateral filter with parameter optimization. By the metrics of PSNR, MSE and accuracy the performance quality is estimated and afterward the outcomes are compared.

Original image The input image is given below as Fig. 2 that is the original data of medical image it get added the noisy after that it becomes noisy signal. Then in Fig. 3 the noisy will be added and then it gets noisy image. The analyses were performed on a few 2D cuts of the recreated cerebrum MR picture in the wake of defiling them by the expansion of Rician commotion with a few clamor differences, specifically, 10, 20 what's more, 30. In our examination, every one of the tests was executed in the MATLAB. Initial, a few introductory tests were performed to decide the fitting EGOA parameters including populace size and age number. Consequently, we utilized a arrangement of mimicked T1-weigthed MR cuts as the base picture and three extra arrangement of loud picture cuts that was produced by the expansion of Rician commotion with three diverse difference esteems including 10, 20 and 30, to the first base picture.

MRI noise characteristics

In MRI, thermal noise is regarded as the vital noise source, which is obtained after the free electrons stochastic motional developments [31]. With zero mean and equivalent variance it can be considered as additive noise, Gaussian distributed noise and white noise. Subsequent to recreating MR image both the imaginary and real parts are influenced by Gaussian noise utilizing IDFT (Inverse Discrete Fourier Transform) of MR information on account of the linearity and orthogonality standards [32]. The remade MR images magnitude is frequently favored for computer examination or visual assessment. Therefore, by a Rician distribution [33] the MRI magnitude esteem acquired is characterized after computing the

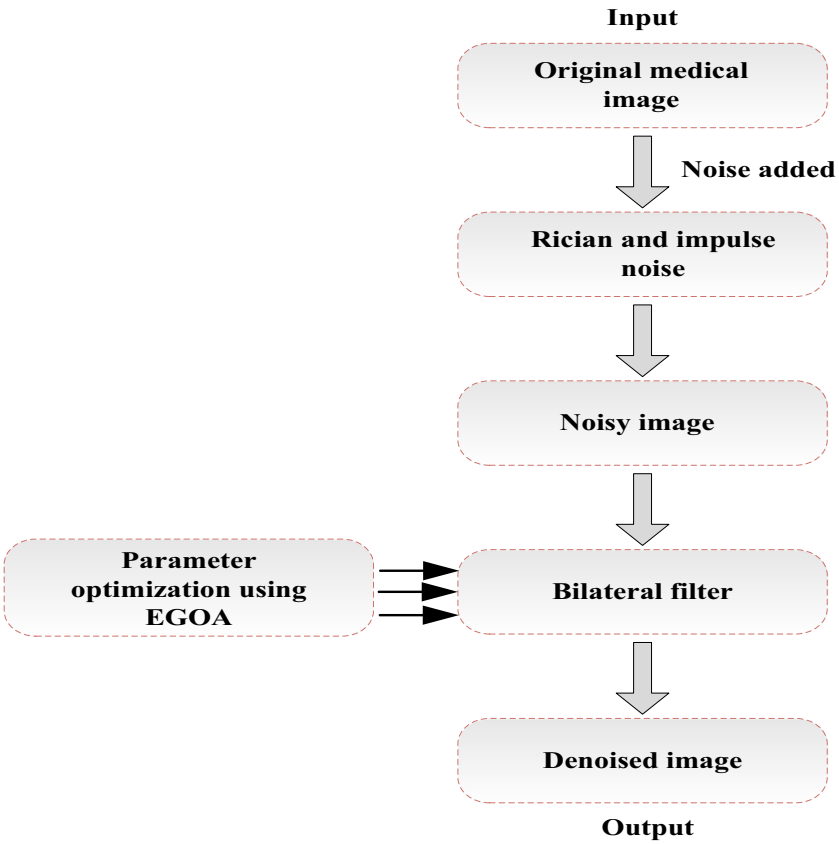

Fig. 1 Proposed methodology

square root of the sum of two independent random Gaussian variables like imaginary and real images. The PDF (probability distribution function) of Rician distributed magnitude information is portrayed as,

$$p_{Magnitude}(m) = \frac{m}{sd^2} e^{-\left(\frac{m^2+a^2}{2sd^2}\right)} i_0\left(\frac{ma}{sd^2}\right) \quad (1)$$

Where, the modified zero-th order first kind Bessel function is denoted as i_0, the pixel intensity of image without noise is $a = \left(\mu_{R_p}^2 + \mu_{I_p}^2\right)^{1/2}$ and the measured intensity of pixels is$m = \left(R_p^2 + I_p^2\right)^{1/2}$. The real and imaginary parts of complex MR data are R_p^2 and I_p^2, incorporates Gaussian noise with *sd* standard deviation and zero mean. Thus, SNR can be

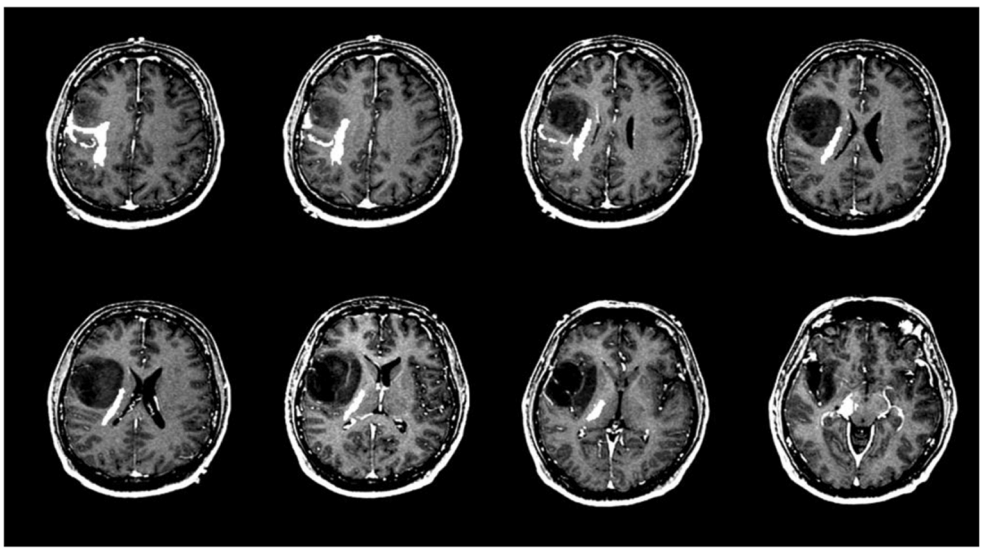

Fig. 2 Input image of the original medical image

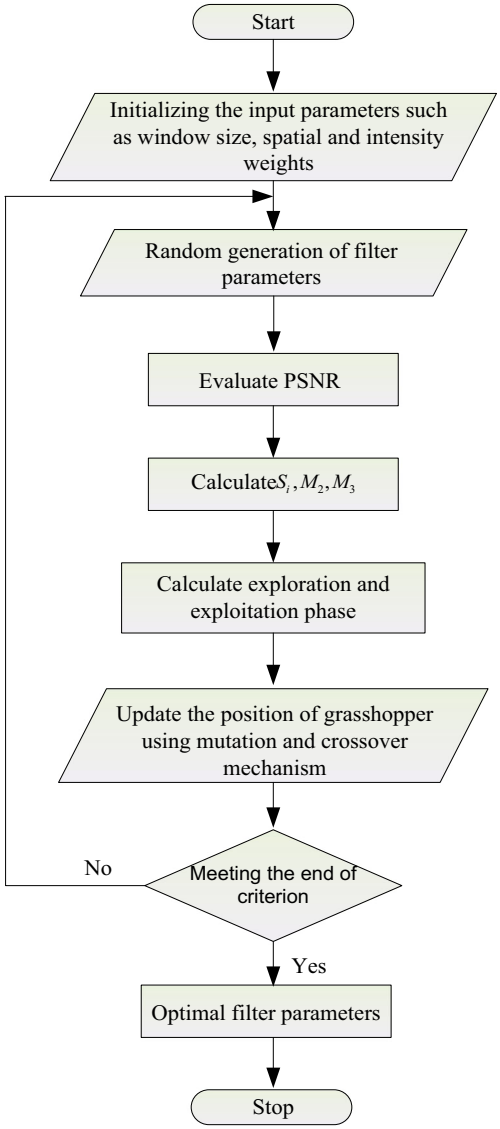

Fig. 3 Flowchart of EGOA iteration procedure

depicted by $^{a}/_{sd}$ and the proportion affects the Rician distribution shape. At the point when the value of SNR goes to zero i.e., low, then Rician distribution starts to become a Rayleigh distribution and the PDF is given by

$$p_{Magnitude}(m) = \frac{m}{sd^2} e^{-\left(\frac{m^2}{2sd^2}\right)} \tag{2}$$

On the other hand the Rician distribution starts to become a Gaussian distribution when the SNR values are high expressed as [33].

$$p_{Magnitude}(m) \approx \frac{1}{\sqrt{2\pi sd^2}} e^{-\left(\frac{m-\sqrt{a^2+sd^2}}{2sd^2}\right)} \tag{3}$$

The impulse noise sometimes observed on image as sparsely occurs black and white pixels. The impulse noise PDF is depicted by

$$p_{Magnitude}(m) = \begin{cases} p_a & for\, m = a \\ p_b & for\, m = b \\ 0 & otherwise \end{cases} \tag{4}$$

Where, p_a and p_b are unipolar noises.

Noise elimination using bilateral filter

Tomasi and Manduchi [36] present the bilateral filter as non-iterative and nonlinear filter for preserving edges while eliminating noise. Neighboring pixel's geometric closeness is considered and their likenesses of gray level. In a local neighborhood, BF computes the weighted sum of pixels. The every pixel's neighbors weighted average is utilized for replacing the pixel. In this computation, around its neighborhood the weights can be acquired by both the spatial and intensity distance of a pixel. In a pixel neighborhood the spatial distance is identified to the domain (spatial) filter coefficients while the range (intensity) filter weights is relative to the pixel radiometric distance. The bilateral filter output is ascertained [15] at a pixel location as,

$$i^{'}(x) = \frac{1}{N_c} \sum_{y \in n(x)} e^{\left(\frac{-\|y-x\|^2}{2sd_d^2}\right)} e^{\left(\frac{-\|i(y)-i(x)\|^2}{2sd_r^2}\right)} i(y) \tag{5}$$

Where, the spatial neighborhood of $i(x)$ is represented as $n(x)$, sd_d and sd_r are the two parameters utilized for controlling the tradeoff of the spatial domain and intensity domains weight. The normalization constant from the above equation is computed as

$$N_c = \sum_{y \in n(x)} e^{\left(\frac{-\|y-x\|^2}{2sd_d^2}\right)} e^{\left(\frac{-\|i(y)-i(x)\|^2}{2sd_r^2}\right)} \tag{6}$$

Therefore, for edge preservation and noise elimination the bilateral filter can be acknowledged as a successful filter unlike traditional filters. Anyway the bilateral filter optimal execution relies on the sd_d, sd_r, and $n(x)$ filter parameters.

Enhanced grasshopper optimization algorithm

The EGOA is a meta- heuristic algorithm, it mimics the grasshopper swarms behavior in nature for solving the optimization issues [34]. The EGOA has the ability to upgrade the unpredictable arrangements underlying and joining to an unrivaled point in the interest space. In proposed algorithm the grasshoppers position in the swarm represents the candidate solution to a given optimization issue. EGOA idea includes original GOA created by new populace position seeking to acquire the best position by using the crossover and mutation mechanism. Grasshoppers have a special method of flying. As per mathematical model, the proposed algorithm movement is

most part affected by three factors such as gravity force, social interaction and wind advection. The steps for EGOA technique is examined underneath.

This area introduces the logic and sequential advancement of EGOAs. In this work, we have complied with the logic of GOA and diminished the parameter (c) in due course of cycles. Be that as it may, with the teaching of the distinctive disordered successions in the safe place decrease parameter "c," is the number of iterations and the broadening excellence of the GOA improve till the last emphasis. To build up the variations, a standardization work is utilized to disperse the successions among most extreme and least inclination before it tends to be one-sided with the parameter c. the numerical articulation for this capacity at any cycle s can be given as

$$M_n(s) = M_n^{max} - \frac{M_n^{max} - M_n^{min}}{S} \times s \tag{7}$$

Where S is the maximum iteration

- ***Step 1: Initialization***

In this progression, introduction of swarm with the input is taken as size of window, spatial weights and intensity weights and the yield as the optimal filter parameters.

- ***Step 2: Random Generation***

In this step, arbitrarily select the parameters of filter and compute the fitness value (PSNR) for each new individual.

$$Fitness \quad Function = PSNR \quad of \quad image \tag{8}$$

- ***Step 3: Social Interaction***

From the propelling power of swarming models of locust, the social interaction is presented. Here, the condition for the social interaction of the grasshopper S_i is planned as takes after,

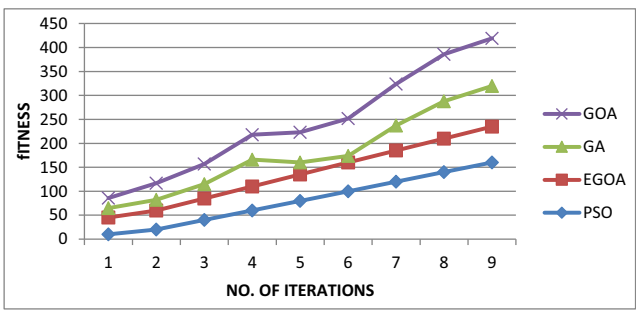

Fig. 4 Performance curve of optimization algorithm

$$S_i = \sum_{\substack{j=1 \\ j \neq 1}}^{n} a_1\left(x_{ij}\right)\overline{x_{ij}} \tag{9}$$

Where, the attraction is communicated as a_1 and grasshopper repulsion is called social interaction, $x_{ij}$is the unit vector of i^{th} grasshopper to the j^{th} grasshopper.

- ***Step 4: Gravity Force***

With the assistance of a_1 function the space between two grasshoppers is arranged into safe place, attraction and repulsion area. The condition for the gravitational consistent M_2 is given as takes after,

$$M_2 = -a_2 U_e \tag{10}$$

Where, the gravitational constant is a_2 and U_e demonstrates the unit vector towards the earth focal point.

- ***Step 5: Wind Advection***

Expect that the wind direction is dependably towards a targeted value (t). The wind advection solution can be formulated as follows,

$$M_3 = -a_3 U_w \tag{11}$$

Where, the constant drift is a_3 and U_w is the unit vector towards the direction of wind.

- ***Step 6: Exploration and Exploitation***

To lessen exploration phase and increase exploitation phase with proportional to the number of iteration, the parameter c is determined with the accompanying equation.

$$c = c_{\max} - iter\left[\frac{c_{\max} - c_{\min}}{n}\right] \tag{12}$$

Where, $c_{\max}$ and $c_{\min}$ are the parameters in the range of 1 and 0.00001, n is the maximum number of iterations, *iter* is the current iteration.

- ***Step 7: Position Updating***

In view of the parameter c esteem the positions of grasshoppers' are updated. In the event that there a superior solution is discovered i.e. $i = i + 1$ update the target solution (t) after the values of c are updated.

- ***Step 8: Crossover and Mutation***

Between two grasshoppers which produce another arrangement of grasshoppers, the crossover rate is accomplished. Into the fitness value of grasshopper and the new produced grasshopper, the procedure is performed. The grasshopper is

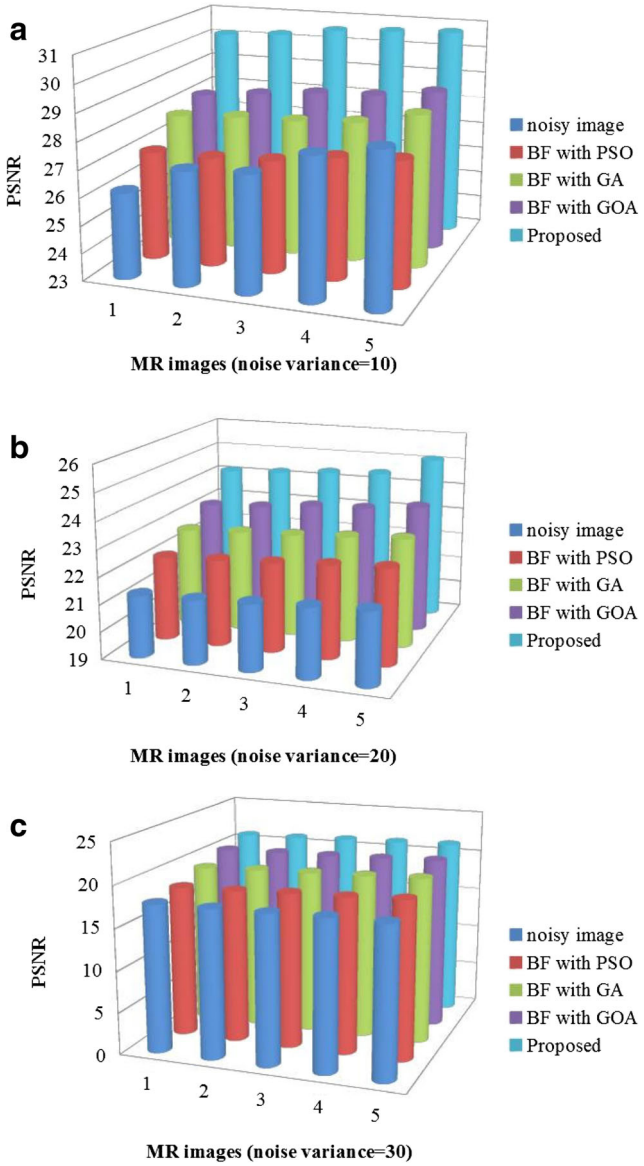

Fig. 5 Comparison of PSNR values of MR images with noise variance **a** 10, **b** 20, **c** 30

randomly mutated in light of the particular mutation rate in the mutation process. For computing the crossover and mutation rate of grasshoppers are calculated based on the accompanying equations: (13, 14):

$$Crossover = \frac{N_{Genes}}{L_{ch}} \tag{13}$$

$$Mutation = \frac{M_p}{L_{ch}} \tag{14}$$

Where, N_{Genes} demonstrates the number of genes crossover, M_p represents the mutation point and L_{ch} indicates the length of chromosome.

- ***Step 9: Termination***

In the termination stage, when the termination criterion is reached, the algorithm completes the technique by giving an optimal solution. Figure 3 shows the flowchart of proposed EGOA procedure.

Parameter selection for BF

The BF execution highly depends on the filter parameters selection. From Eq. (5), it can be showed that $n \times n$ neighborhood window size and sd_d, sd_r the coefficients of Gaussian kernel which adjusts the weights of spatial and intensity parameters can influence the filtered image. Therefore, for controlling both noise elimination and edge preservation all of these parameters must be properly selected. Using a EGOA based optimization procedure these filter coefficients were determined in this paper. Initially, the filter coefficients like spatial and intensity weights, window size were included as genes in an individual to show an optimum solution. Then, it was determined to use the PSNR calculation as the principal function of the EGOA strategy. Thus, calculating the image PSNR value the fitness value for any individual was obtained.

Result and discussion

For MRI investigation noise elimination is an imperative pre-processing step. Subsequent to filtering both the decrease in noise and preservation of edge in unique noisy images are wanted conditions. Identified with this tradeoff there have been numerous procedures between edge preservation and elimination of noise in medical images. This paper we utilize bilateral filter for MR images noise elimination. In the filter, the window size parameters and coefficients of kernel influence the exhibitions of smoothing and filtering. Along these lines, for optimal coefficients assurance in this paper EGOA based novel system is actualized. The yield images PSNR esteems help the reasonable BF parameters modification. With the most noteworthy PSNR esteem the real numbers prompt yield filtered images development, were chosen as the BF parameters best qualities. Also, the extra performance measures, for example, MSE, SSIM PSNR, SNR, and accuracy esteems were utilized as the entire filtering framework. The theoretical explanation of the proposed method is giving the original of medical image and the image will add the noise and get the noisy signal into denoising image then the image is find the evaluation metrics of the signals and the accuracy, computational time all are calculated and compared with the existing methods and the proposed methods. The comparison of the parameter is analyzed and the proposed method gets better value.

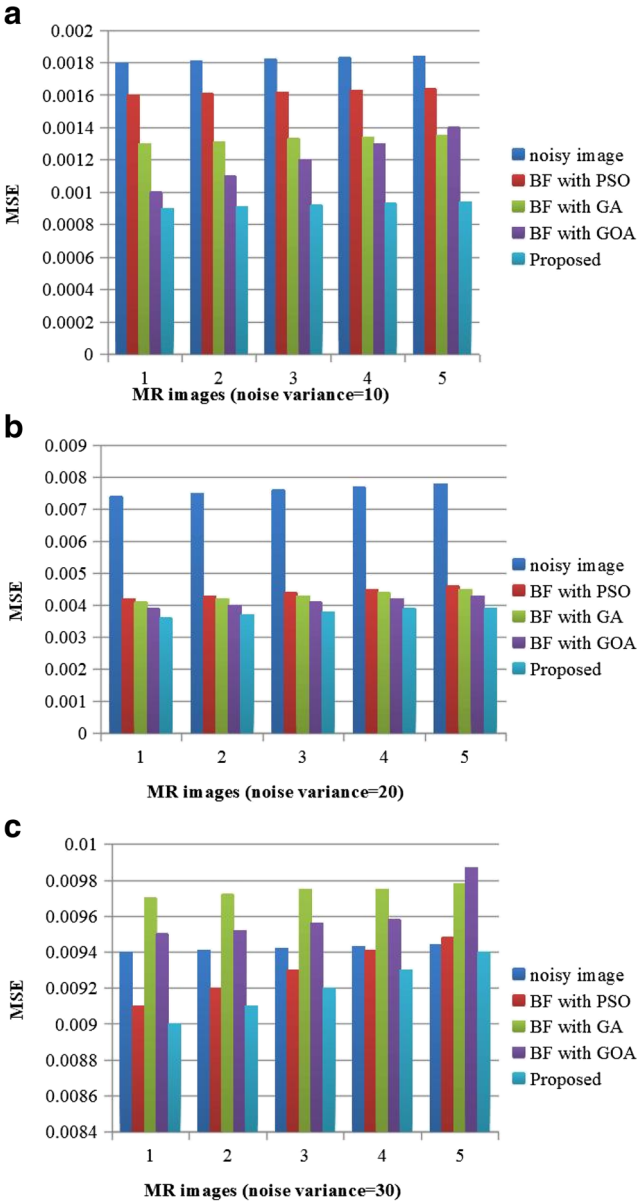

Fig. 6 Comparison of MSE values of MR images with noise variance **a** 10, **b** 20, **c** 30

Dataset description

With intensity values in the range between 0 and 255 the examinations were led on simulated and standard medical MR picture (T1-weighted) slices downloaded from the web database [35]. The extent of image utilized in the trials was $181 \times 217 \times 181$. The MR images ($i_0$) recreated were undermined by noise including as takes after [32]. The noisy image is communicated in condition (15).

$$i_{noisy} = \sqrt{i_r^2 + i_i^2} \tag{15}$$

Where, $i_r = i_0 + \eta_1$, $\eta_1 \approx n(0, sd)$ and $i_1 = \eta_2$, $\eta_2 \approx n(0, sd)$.

Table 1 Optimal BF parameters obtained by proposed method

BF parameters	Sd = 10	Sd = 20	Sd = 30
$n \times n$	7 × 7	7 × 7	3 × 3
sd_d	0.806	1.068	1.553
sd_r	0.167	0.227	0.236

Evaluation metrics

To assess the bilateral filter parameters result selected utilizing EGOA measurements such as MSE, PSNR, RMSE, SSIM and accuracy were ascertained.

Mean squared error

The first measure is MSE which show the difference between two images as

$$MSE_{measure} = \frac{1}{RC} \sum_{r=0}^{R-1} \sum_{c=0}^{C-1} \left[i_0(r,c) - i_{noisy}(r,c) \right]^2 \tag{16}$$

Where, the noise less original image is i_0, the noisy image is represented as i_{noisy}, the number of rows and columns are denoted as R and C respectively.

Peak signal to noise ratio

As per the original image the PSNR reflects the evaluated image quality by the two images target contrast and the PSNR is characterized as,

$$PSNR_{measure} = 10 \times \log_{10} \frac{n^2}{MSE} \tag{17}$$

Here, the number of image gray levels is n.

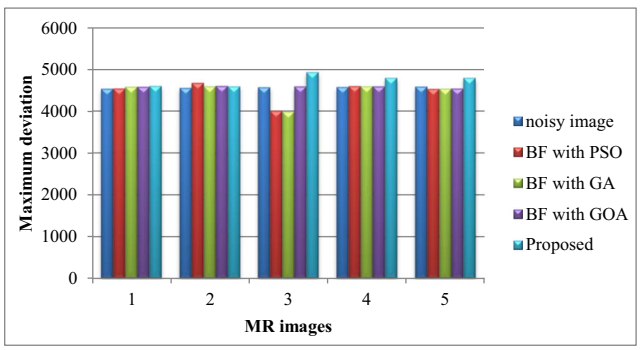

Fig. 7 Maximum deviation analysis of five medical MR images

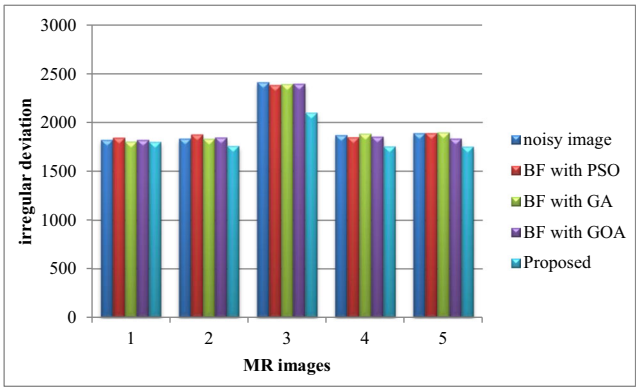

Fig. 8 Irregular deviation analysis of five medical MR images

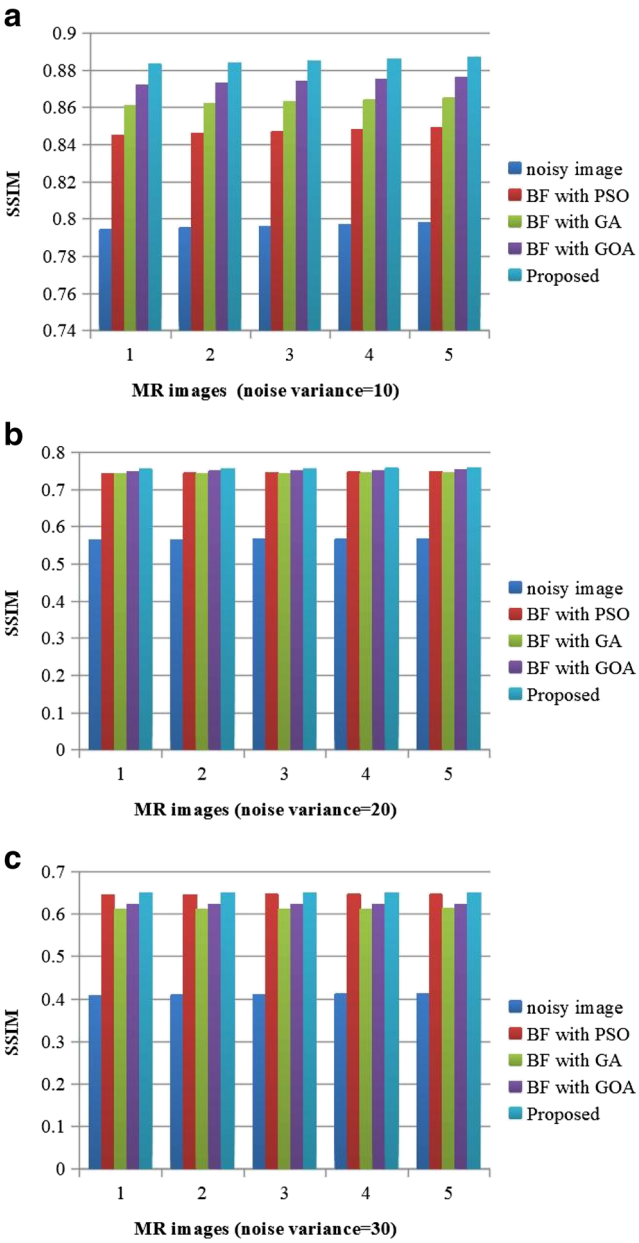

Fig. 9 Evaluation chart of SSIM values of MR images with noise variance **a** 10, **b** 20, **c** 30

Signal to noise ratio

The another measure SNR gives a connection between the evaluated and original image which is computed as

$$SNR_{measure} = 10 \times \log_{10} \frac{\left({}^{1}/_{RC}\right) \sum_{c=0}^{C-1} (i_0)^2 (r,c)}{MSE} \tag{18}$$

Structural similarity index metric

For finding the comparability (similarity) between two images (X, Y) the SSIM measure is characterized as

$$SSIM_{measure}(X,Y) = \frac{(2\mu_X\mu_Y + a_1)(2sd_{XY} + a_2)}{(\mu_X{}^2 + \mu_Y{}^2 + a_1)(s, d_X^2, +, s, d_Y^2, +, a_2)} \tag{19}$$

Where, the average of X is μ_X, the average of Y is μ_Y, a_1 and a_2 are constants, the variances of X and Y are sd_X^2 and sd_X^2, the covariance of X and Y are signified as sd_{XY}.

Accuracy

The degree in which data in a computerized database coordinates its actual values is called accuracy. The accuracy measure near the real value and it is a true outcomes proportion processed as

$$accurarcy = \frac{T_P + T_N}{T_P + T_N + F_P + F_N} \tag{20}$$

Where, T_P and T_N are the true positive and true negative of images. F_P and F_N are the false positive and false negative of MR images.

In the Fig. 4 it shows the performance curve of the EGOA and all existing optimization algorithm. The proposed method gives a better fitness value. The performance is increased in the robust model.

Comparison of quantitative metrics

The experiments were performed on few simulated medical MR image after corrupting then by expansion of noises with few noise variances for example 10, 20 and 30. Also, the three arrangement containing noises with variances (10, 20, and 30) with five MR images were fed to the EGOA procedure to search for the best BF parameters for the similar MR images in tests that offered ascend to the output images development with the highest possible PSNR value.

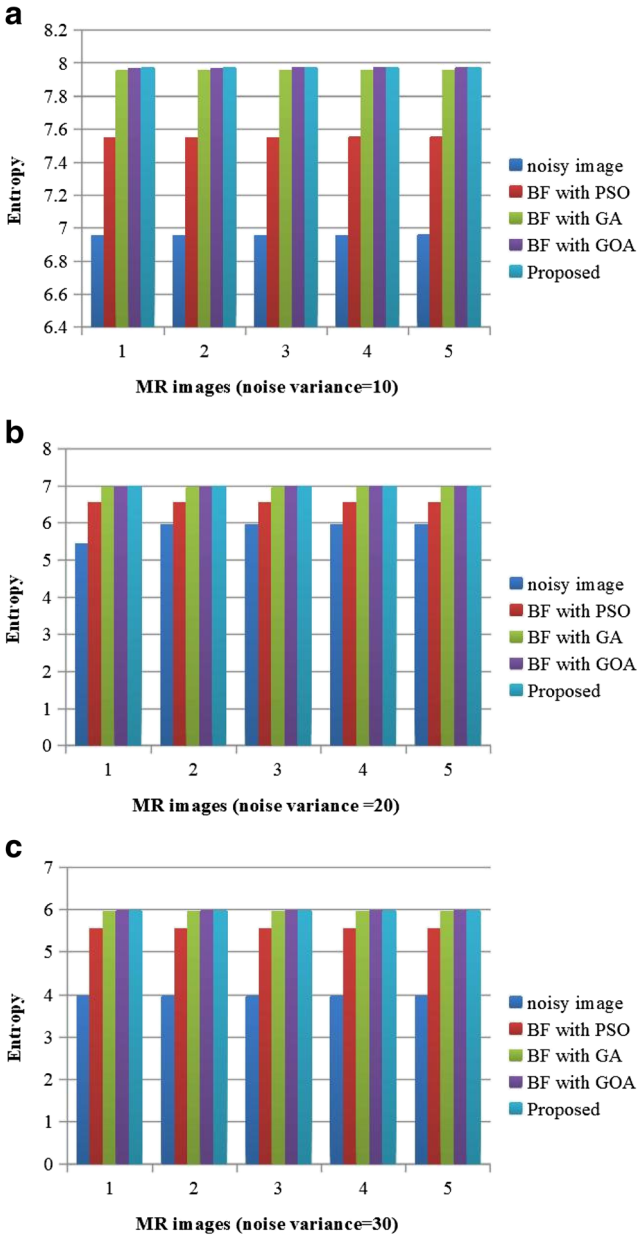

Fig. 10 Comparison of Entropy values of MR images with noise variance **a** 10, **b** 20, **c** 30

Figure 5 demonstrates the comparison of PSNR values that were acquired for proposed and other methods. The PSNR values for noisy images are 27.4 for 10 noise level, 21.28 for 20 noise level and 17.69 for 30 noise level. We found the best PSNR values for proposed denoised method to be 30.142, 24.35 and 20.46 for noise levels of 10, 20, and 30 separately when contrasted with other denoised strategies.

The examination of MSE values with noisy and denoised images is shown in Fig. 6. As found in Fig. 6 the MSE of the proposed method is bring down when contrasted with BF with PSO, BF with GA, BF with GOA and noisy image.

The optimal bilateral filter parameters obtained by proposed EGOA based computation to denoise the MR image corrupted with various Rician noise variances is appeared in Table 1. The window size parameter of the BF could expect just the value in [7 × 7, 3 × 3] ranges with spatial and intensity sigma parameters values. For instance, by the proposed method the best PSNR values are obtained for the filter parameters with window size as 7 × 7, sd_d as 0.806, sd_r as 0.167 with sd = 10 in the noisy image.

The maximum deviation of medical MR images are shown in Fig. 7 and the irregular deviation of the five MR images are shown in Fig. 8. From the analysis, it is evident that the proposed EGOA provides maximum deviation and minimum irregular deviation when compared with the conventional method.

In this Fig. 7 the maximum deviation analysis of five medical MR images is given for the existing and the proposed method. In this the proposed method gets high and better deviation while comparison.

The Fig. 8 gives the irregular deviation of five images in that our proposed gets better deviation all the other existing gets high irregular deviation. The results of PSNR, MSE and SSIM of the bilateral filter with optimized parameters outperform other three methodologies. The denoised image PSNR and SSIM have expanded to higher reaches for each noise level giving better expulsion in noise with high quality image. In addition, from the denoised images the lower MSE values were obtained with our proposed method. Comparison of SSIM values of noisy and

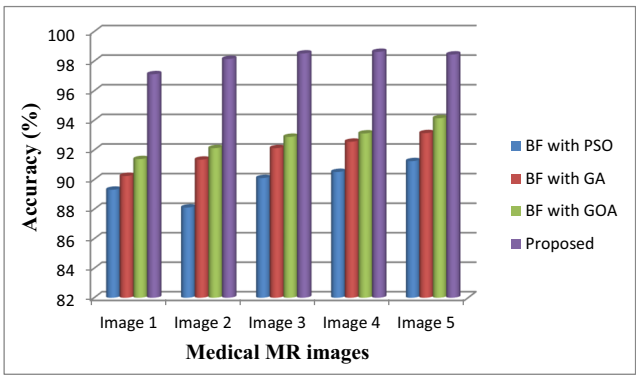

Fig. 11 Accuracy of various methodologies

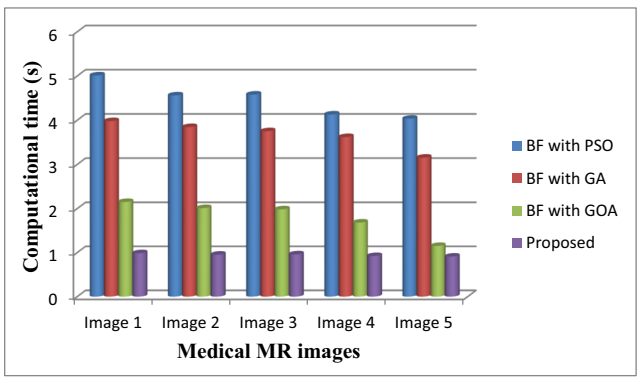

Fig. 12 Computational time of simulated medical MR image during denoising process

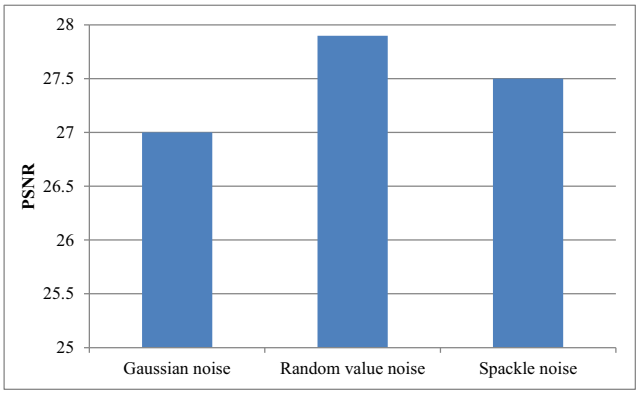

Figure 13 comparison between different noises

denoised image with different noise levels is appeared in Fig. 9. The proposed method gets better value in the chart while comparing the existing methods.

Figure 10 shows the determination of entropy for five medical MR images. The analysis among the figure indicates that the information entropy is high for the proposed EGOA than the conventional methods.

The Figs. 11 and 12 shows the accuracy and the computational values. The accuracy of our method is gets high value and the accuracy is nearly equal to the 100%. The computational time of our proposed method is very low while comparing the existing methods. Notwithstanding evaluation metrics the taken for our proposed technique in simulated images for elimination of noise was computed and contrasted with other methodologies with various setting of parameters, which is shown in Fig. 8. At that point examine the parameter estimation adequacy for bilateral filter by various optimization approaches, it is evident that both the GA and GOA techniques gives same output in terms of accuracy yet the proposed technique has high accuracy. Figure 9 demonstrates the execution time of different parameter enhancement. In this manner alluding to the correlations, it is evident that under various noise variance bilateral filter with proposed optimization method works better than bilateral filter applied to other optimizations. Thus the noisy medical MR images were denoised efficiently utilizing the proposed strategy and preserving the visual nature of image. Figure 13 shows the comparison between three different noises like Gaussian noise, Random valued noise and Spackle noise using bilateral filter [37].

Conclusion

In this paper, we proposed an EGOA based method as a novel way for choosing bilateral filter parameters to expel impulse and Rician noise in medical MR images. Although there are sufficient number of works that compare the diverse optimization approaches effectiveness such as PSO, GA, and GOA. In order to comprehend the BF parameter selection importance we compared the denoising results based on parameters proposed with other results of already proposed parameters utilizing different assessment measurements like PSNR, SNR, MSE, SSIM and accuracy. Besides, while removing noise it secures the details of image better. The bilateral filter with proposed optimal parameter accomplished better exhibitions for all the images with various noises in all quality measures.

Compliance with ethical standards

Conflict of interest V. Anoop declares that he has no conflict of interest. Bipin PR declares that he has no conflict of interest.

Ethical approval This article does not contain any studies with human participants or animals performed by any of the authors.

References

1. R. Biswas, D. Purkayastha and S. Roy, Denoising of MRI Images Using Curvelet Transform. Advances in Systems, Control and Automation, pp. 575–583, 2017.
2. Jifara, W., Jiang, F., Rho, S., Cheng, M., and Liu, S., Medical image denoising using convolutional neural network: a residual learning approach. J. Supercomput., 2017.
3. Ben Said, A., Hadjidj, R., and Foufou, S., Total Variation for Image Denoising Based on a Novel Smart Edge Detector: An Application to Medical Images. Journal of Mathematical Imaging and Vision, 2018.
4. K. Das, M. Maitra, P. Sharma and M. Banerjee, Early Started Hybrid Denoising Technique for Medical Images. Recent Trends in Signal and Image Processing, pp. 131–140, 2018.
5. Lysaker, M., Lundervold, A., and Tai, X.-C., Noise removal using fourth-order partial differential equation with applications to medical magnetic resonance images in space and time. IEEE Trans. Image Process. 12(12):1579–1590, 2003.
6. Arora, S., Hanmandlu, M., and Gupta, G., Filtering impulse noise in medical images using information sets. Pattern Recogn. Lett., 2018.
7. Bai, J., Song, S., Fan, T., and Jiao, L., Medical image denoising based on sparse dictionary learning and cluster ensemble. Soft. Comput. 22(5):1467–1473, 2017.
8. Lee, Y., Improved total-variation noise-reduction technique with gradient method using iteration counter and its application in medical diagnostic chest and abdominal X-ray imaging. Optik 170: 475–483, 2018.
9. Caldairou, B., Passat, N., Habas, P., Studholme, C., and Rousseau, F., A non-local fuzzy segmentation method: Application to brain MRI. Pattern Recogn. 44(9):1916–1927, 2011.
10. Yang, J., Fan, J., Ai, D., Wang, X., Zheng, Y., Tang, S., and Wang, Y., Local statistics and non-local mean filter for speckle noise reduction in medical ultrasound image. Neurocomputing 195:88–95, 2016.
11. Gai, S., Zhang, B., Yang, C., and Yu, L., Speckle noise reduction in medical ultrasound image using monogenic wavelet and Laplace mixture distribution. Digital Signal Processing 72:192–207, 2018.
12. Sudeep, P., Palanisamy, P., Rajan, J., Baradaran, H., Saba, L., Gupta, A., and Suri, J., Speckle reduction in medical ultrasound

images using an unbiased non-local means method. Biomedical Signal Processing and Control 28:1–8, 2016.
13. Zhang, Y., Tian, X., and Ren, P., An adaptive bilateral filter based framework for image denoising. Neurocomputing 140:299–316, 2014.
14. Qi, M., Zhou, Z., Liu, J., Cao, J., Wang, H., Yan, A., Wu, D., Zhang, H., and Tang, L., Image Denoising Algorithm via Spatially Adaptive Bilateral Filtering. Adv. Mater. Res. 760-762:1515–1518, 2013.
15. Zhang, M., and Gunturk, B., Multiresolution Bilateral Filtering for Image Denoising. IEEE Trans. Image Process. 17(12):2324–2333, 2008.
16. Ramanandan, S., Lehmann, B., and Kraus, D., Optimal parameters for bilateral filtering and SAS image denoising. 2011 International Symposium on Ocean Electronics, 2011.
17. Shi, H., Determination of bilateral filter coefficients based on particle swarm optimization. 2012 5th International Congress on Image and Signal Processing, 2012.
18. Borntrager, C., Chorpita, B., Orimoto, T., Love, A., and Mueller, C., Validity of Clinician's Self-Reported Practice Elements on the Monthly Treatment and Progress Summary. The Journal of Behavioral Health Services & Research 42(3):367–382, 2013.
19. Farooq, M., Application of Genetic Algorithm & Morphological Operations for Image Segmentation. IJARCCE:195–199, 2015.
20. Hu, K., Cheng, Q., Li, B., and Gao, X., The complex data denoising in MR images based on the directional extension for the undecimated wavelet transform. Biomedical Signal Processing and Control 39:336–350, 2018.
21. Sharif, M., Arfan Jaffar, M., and Tariq Mahmood, M., Optimal composite morphological supervised filter for image denoising using genetic programming: Application to magnetic resonance images. Eng. Appl. Artif. Intell. 31:78–89, 2014.
22. Özmen, G., and Özşen, S., A new denoising method for fMRI based on weighted three-dimensional wavelet transform. Neural Comput. & Applic. 29(8):263–276, 2017.
23. Malik, M., Ahsan, F., and Mohsin, S., Adaptive image denoising using cuckoo algorithm. Soft. Comput. 20(3):925–938, 2014.
24. de Paiva, J., Toledo, C., and Pedrini, H., An approach based on hybrid genetic algorithm applied to image denoising problem. Appl. Soft Comput. 46:778–791, 2016.
25. Zhang, J., Lin, G., Wu, L., and Cheng, Y., Speckle filtering of medical ultrasonic images using wavelet and guided filter. Ultrasonics 65:177–193, 2016.
26. Miri, S. S., Rashidi, S., and Ghods, M., Medical image denoising based on 2D discrete cosine transform via ant colony optimization. Optik 156:938–948, 2018.
27. Naimi, H., Adamou-Mitiche, A., and Mitiche, L., Medical image denoising using dual tree complex thresholding wavelet transform and Wiener filter. Journal of King Saud University - Computer and Information Sciences 27(1):40–45, 2015.
28. Marschner, H., Pampel, A, and Moeller, H., Method and device for magnetic resonance imaging with improved sensitivity by noise reduction. U.S. Patent Application No. 15/572,009, 2018.
29. Sudeep, P. V. et al., An improved nonlocal maximum likelihood estimation method for denoising magnetic resonance images with spatially varying noise levels. Pattern Recogn. Lett., 2018.
30. Chen, G. et al., Noise reduction in diffusion MRI using non-local self-similar information in joint x− q space. Med. Image Anal. 53: 79–94, 2019.
31. Riji, R., Rajan, J., Sijbers, J. and Nair, M., Iterative bilateral filter for Rician noise reduction in MR images, 2018.
32. Sijbers, J., den Dekker, A., Van Audekerke, J., Verhoye, M., and Van Dyck, D., Estimation of the Noise in Magnitude MR Images. Magn. Reson. Imaging 16(1):87–90, 1998.
33. Gudbjartsson, H., and Patz, S., The Rician distribution of noisy MRI data. Magn. Reson. Med. 34(6):910–914, 1995.
34. Mirjalili, S., Saremi, S., Faris, H., and Aljarah, I., Grasshopper optimization algorithm for multi-objective optimization problems. Appl. Intell. 48(4):805–820, 2017.
35. Medical MR image database: https://github.com/sfikas/medical-imaging-datasets
36. Tomasi, C., Manduchi, R., Bilateral filtering for gray and color images. In: *Computer Vision, 1998. Sixth International Conference on,* (pp. 839–846). IEEE, 1998.
37. Bhonsle, D., Chandra, V., and Sinha, G. R., Medical image denoising using bilateral filter. International Journal of Image, Graphics and Signal Processing 4(6):36, 2012.